

# Two-Dimensional Infrared (2DIR) Spectroscopy of the Peptide Beta3s Folding

Zaizhi Lai,<sup>†</sup> Nicholas K Preketes,<sup>§</sup> Jun Jiang,<sup>||</sup> Shaul Mukamel,<sup>§</sup> and Jin Wang<sup>\*,†,||,⊥</sup>

<sup>†</sup>Department of Chemistry and <sup>‡</sup>Department of Chemistry, Department of Physics and Astronomy, State University of New York at Stony Brook, Stony Brook, New York 11794, United States

<sup>§</sup>Department of Chemistry, University of California, Irvine, California 92697-2025, United States

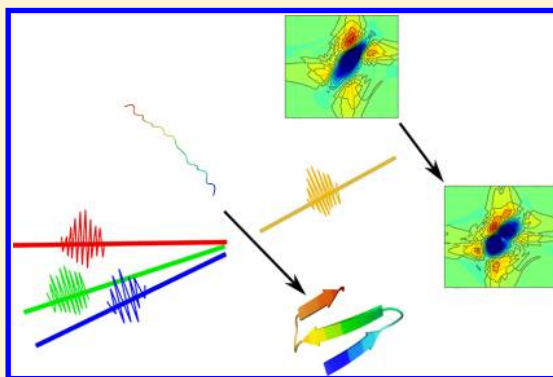
<sup>||</sup>Department of Chemical Physics, University of Science and Technology of China, Hefei, Anhui 230026, P. R. China

<sup>⊥</sup>State Key Laboratory of Electroanalytical Chemistry, Changchun Institute of Applied Chemistry, Chinese Academy of Sciences, Changchun 130022, P. R. China

## S Supporting Information

**ABSTRACT:** Probing the underlying free-energy landscape, pathway, and mechanism is the key to understanding protein folding in theory and experiment. Time-resolved two-dimensional infrared (2DIR) with femtosecond laser pulses has emerged as a powerful tool for investigating the protein folding dynamics on much faster time scales than possible by NMR. We have employed molecular dynamics simulations to compute 2DIR spectra of the folding process of a peptide, Beta3s. Simulated nonchiral and chiral 2DIR signals illustrate the variation of the spectra as the peptide conformation evolves along the free-energy landscape. Chiral spectra show stronger changes than the nonchiral signals because cross peaks caused by the formation of the  $\beta$ -sheet are clearly resolved. Chirality-induced 2DIR may be used to detect the folding of  $\beta$ -sheet proteins with high spectral and temporal resolution.

**SECTION:** Spectroscopy, Photochemistry, and Excited States



The energy landscape theory provides an essential framework for understanding protein folding and has been widely used to interpret the folding process.<sup>1–3</sup> The theory assumes a funnel-like shape of the surface, which is sufficiently biased to direct the folding so that the native state can be reached on the experimental time scale. Monitoring conformational changes of proteins is important for understanding the details of energy landscape and uncovering the mechanism of folding process. There are a limited number of effective probes that can detect structural evolution on the time scales of folding dynamics. Commonly used spectroscopic techniques such as NMR, due to limited millisecond time resolution, may not directly trace the faster dynamical process. Two-dimensional infrared (2DIR) spectroscopy provides a promising avenue to investigate protein folding dynamics down to 100 fs resolution.<sup>4–6</sup> In 2DIR experiments, the amide I band, associated with the peptide bond carbonyl stretch, is by far the most studied because of its sensitivity to hydrogen bonding, dipole–dipole interactions, and geometry of the peptide backbone, thus providing a good indicator of secondary structure. The cross peaks in 2DIR spectra provide signatures of intra- and intermolecular couplings, providing additional structural information not available in linear spectroscopy. Here we report simulations of 2DIR spectra of the folding of Beta3s

on the free-energy landscape. Beta3s is a 20 amino acid peptide (Thr1-Trp2-Ile3-Gln4-Asn5-Gly6-Ser7-Thr8-Lys9-Trp10-Tyr11-Gln12-Asn13-Gly14-Ser15-Thr16-Lys17-Ile18-Tyr19-Thr20), and NMR experiments have shown that it folds into a single structured compact form, the three-stranded antiparallel  $\beta$ -sheet conformation with turns at Gly14-Ser15 and Gly6-Ser7, in equilibrium solution.<sup>7</sup>

We have applied a molecular dynamics (MD) protocol to simulate the folding dynamics of the peptide. We used the CHARMM c35b5 package<sup>8</sup> with the TOPH19/PARAM19 parameter set<sup>9</sup> to perform all MD simulations and part of the analysis. The folding simulations were performed with an implicit solvent model.<sup>10</sup> Honig et al. have suggested that the van der Waals and hydrophobic interactions are the primary factors which determine the stability of  $\beta$ -sheet proteins.<sup>11</sup> Also, recent studies<sup>12,13</sup> imply that the contacts between side chains are responsible for driving the folding of peptide with antiparallel  $\beta$  sheets, suggesting that the use of an implicit solvent does not significantly influence the folding process. The nonbonded interaction list was extended to cut off as 7.5 Å, and

**Received:** March 18, 2013

**Accepted:** May 20, 2013

**Published:** May 20, 2013

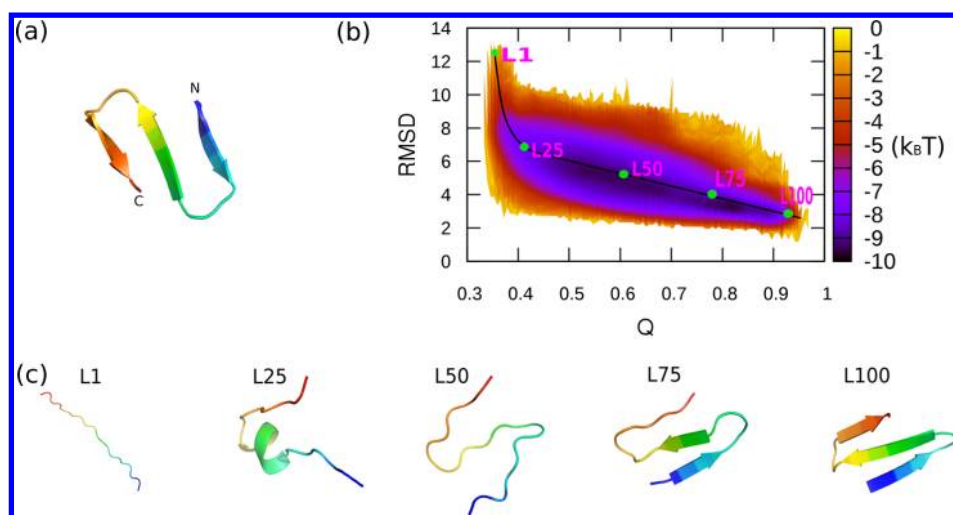


**Figure 1.** (a) Native structure from model 1 of the NMR structures.<sup>7</sup> (b) Free-energy profile of Beta3s folding as a function of RMSD (Å) from the native structure and the fraction of native contacts. Five locations on the folding pathway are indicated. (c) Corresponding structures of the five locations.

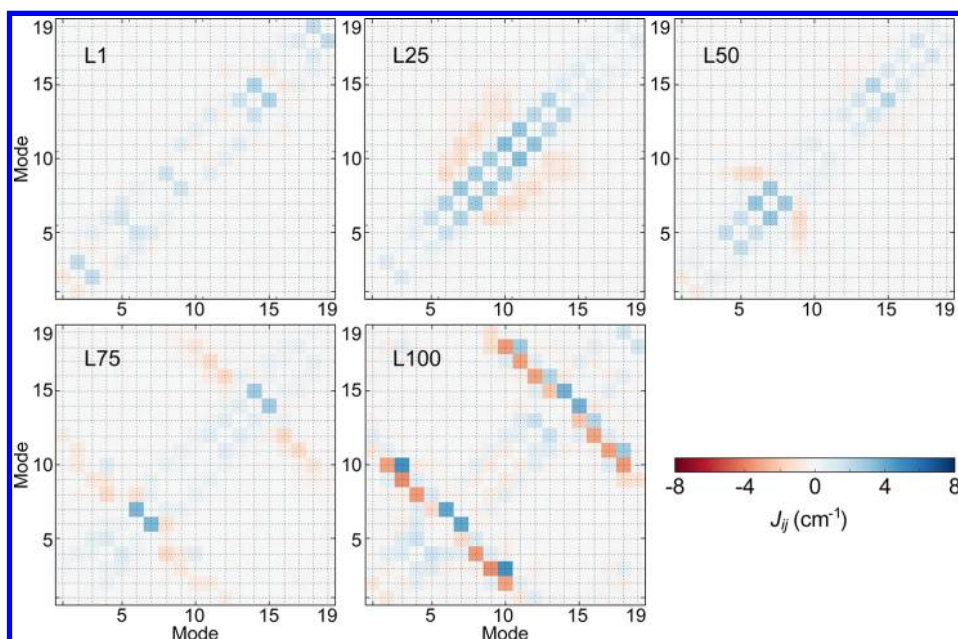


**Figure 2.** Average dipole–dipole coupling between the amide I vibrational modes at L1, L25, L50, L75, and L100.

all covalent bond lengths including hydrogen atoms were fixed with the SHAKE algorithm.<sup>14</sup> From the native structure, 20 trajectories were simulated at 330 K for 500 ns. The total 10  $\mu$ s folding simulation trajectories provided sufficient data to build up the free-energy landscape, which is a function of RMSD (root-mean-square deviation) and  $Q$  (fraction of native contacts of  $C_\alpha$  atoms). The native contacts are listed in Table 1 in the Supporting Information, and a contact was defined as formed when its pair distance falls within a range  $r_{\text{native}} \pm 2$  Å, where  $r_{\text{native}}$  is the distance of that contact in the native structure. Along the dominant folding pathway, 100 locations were selected on the energy landscape. The distance between any two adjacent locations was moderate so that these locations can well-characterize the entire pathway.

The simulation protocol of amide I linear absorption and 2DIR spectra has been discussed in detail elsewhere.<sup>15</sup> The map of ref 16 was used to model the fluctuating amide I frequencies,

while the anharmonicity was fixed to  $-16$   $\text{cm}^{-1}$ . The nearest-neighbor couplings were given by the Torii and Tasumi dihedral angles map,<sup>17</sup> while all other couplings were calculated using the transition dipole coupling formula.<sup>17</sup> All simulations were performed in a homogeneous dephasing of 5.5  $\text{cm}^{-1}$  and impulsive pulses. Static (inhomogeneous) averaging was performed. The absorptive ( $k_1 + k_{11}$ ) 2DIR spectra were simulated for five locations (L1, L25, L50, L75, L100) on the free-energy landscape. At each location, the spectrum was averaged over 150 conformations. Each conformation was explicitly solvated in TIP3P<sup>18</sup> water and equilibrated for 10 ps prior to calculating the fluctuating parameters in the excitonic Hamiltonian. Spectra were simulated for the nonchiral (i.e.,  $xxxy$ ) and chirality-induced (CI) (i.e.,  $xxxxy$ ) polarization configurations, where  $ijkl$  indicates the pulse polarization in chronological order.



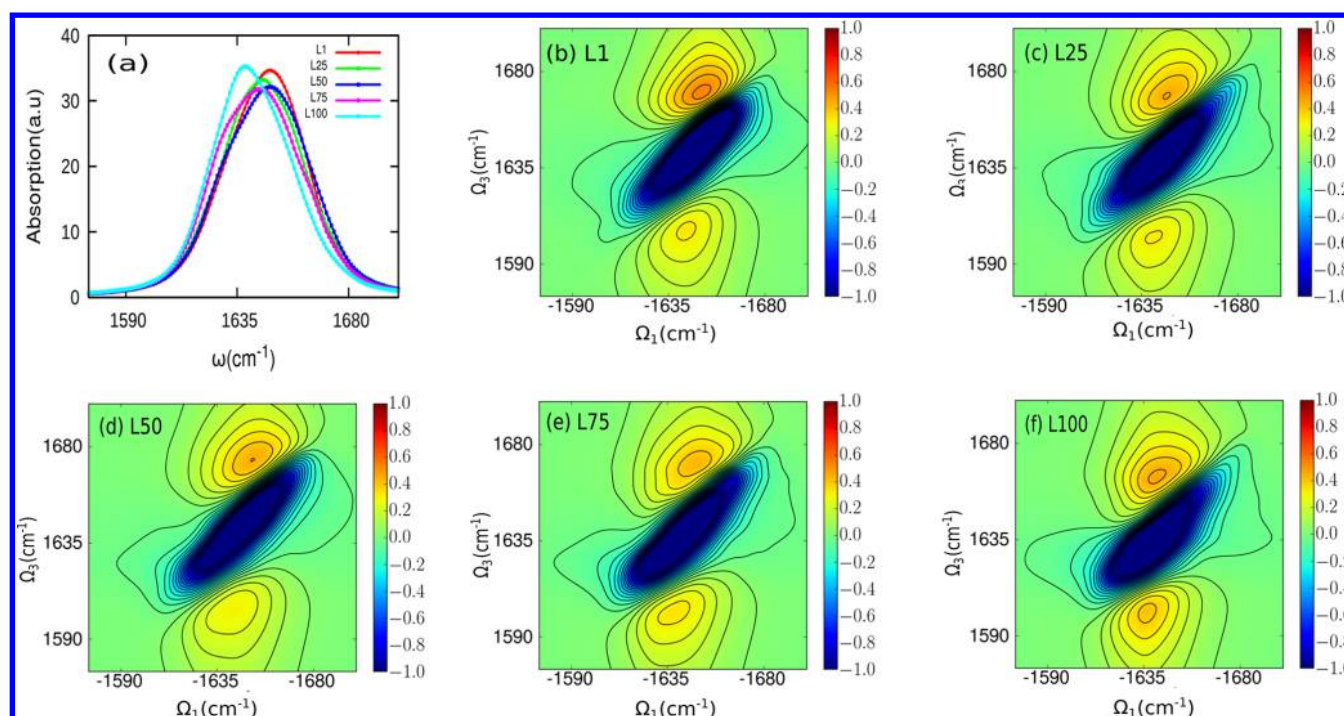


**Figure 3.** (a) Linear absorption spectra of the locations L1, L25, L50, L75, and L100. (b–f) Nonchiral (xxxy) 2DIR signals of the same locations. The 2D spectra were plotted by using arcsinh scale.<sup>29</sup>

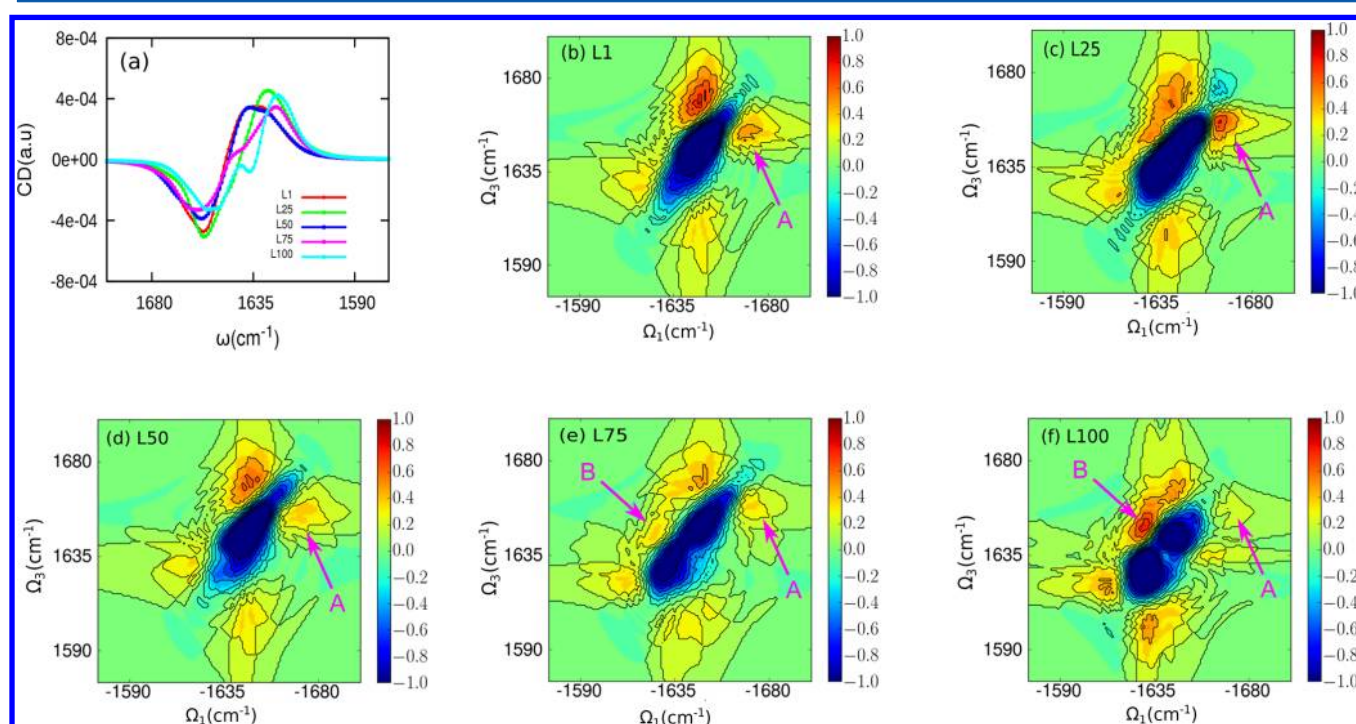


**Figure 4.** (a) VCD spectra and (b–f) chiral 2DIR spectra of the locations L1, L25, L50, L75, and L100. The 2D spectra were plotted by using arcsinh scale.<sup>29</sup> Peaks A and B are labeled by pink arrows.

Figure 1b shows the free-energy landscape of Beta3s folding plotted as a function of the RMSD and  $Q$ . A one-dimensional free energy profile as a function of RMSD is included in the Supporting Information.) The free-energy profile was obtained by  $F = -\log(P)$ , where  $P$  is the statistical population obtained from the 10  $\mu\text{s}$  MD simulated data. At L1, the peptide has an extended structure. At L25, the termini have random-coil

structures, yet residues 8–13 formed a short  $\alpha$ -helix. At L50, the short  $\alpha$ -helix reopened and the orientations of three strands formed. Between L50 and L75, we witnessed the formation of two  $\beta$  strands. L100 was the folded state, which consisted of three antiparallel  $\beta$  sheets. This folding scenario is consistent with a previous study.<sup>19</sup>

The transition dipole couplings are displayed in Figure 2 to demonstrate the structural changes that occur during folding. At L1, the coupling is weak and is dominated by nearest-neighbor couplings. This is indicative of a random coil. At L25, a short  $\alpha$ -helix forms from residues 8 to 13, as seen by the strong positive nearest neighbor coupling and the strong negative 1–3 coupling in this region.<sup>20–22</sup> When the peptide arrives at L50, the helical structure opens and the couplings between residues 8–13 decrease. From L75, as the orientations of three strands form and the peptide folds to the native state, the couplings between residues 1–5 and 8–12 and the couplings between residues 8–12 and 16–20 are enhanced, clearly indicating the formation of the antiparallel  $\beta$ -sheet structure. These couplings strengthen as the peptide evolves from L75 to the stable folded state at L100. The couplings  $J_{ij}$  (Figure 2) will now be used, as input to the system Hamiltonian, to calculate the infrared absorption, vibrational circular dichroism (VCD), and nonchiral and chiral 2DIR spectra. As we will show, these couplings manifest themselves as cross peaks in the 2DIR spectra.

Figure 3a shows the infrared absorption spectra of the five locations along the folding pathway. They all have one major peak, which red shifts from 1645  $\text{cm}^{-1}$  at L1 to 1630  $\text{cm}^{-1}$  at L100. This red shift is consistent with previous studies on similar systems.<sup>23–28</sup>

Figure 3b–f shows the real part of the absorptive 2D  $xyxy$  spectra. All spectra are dominated by an inhomogeneously (diagonally) broadened peak. The inhomogeneous distribution and the homogeneous dephasing, which were used to compute the spectra, largely determined the peak shape. Compared with L1, the diagonal L100 peak is red-shifted around 10  $\text{cm}^{-1}$  (from 1645 to 1630  $\text{cm}^{-1}$ ), consistent with the above linear absorption spectrum. The similarity of the 2DIR  $xyxy$  spectra indicates that the  $xyxy$  spectra are not very sensitive to protein secondary structure. This motivates the study of exploring more sensitive probes such as chiral 2DIR spectra.

The VCD and CI 2DIR spectra are shown in Figure 4. The VCD spectra (Figure 4a) for all locations have a positive couplet (+ peak, followed by – peak with increasing frequency). The positive peak is red-shifted by  $\sim 10 \text{ cm}^{-1}$  from L1 to L100 as the  $\beta$ -sheet structure forms. The intensity of the positive peak increases slightly from L1 to L25. From L50 to L100, the intensities of both peaks slightly increase as the planar antiparallel  $\beta$ -sheet forms. The VCD spectrum at L100 agrees well with the ab initio simulated VCD spectrum of a three-stranded planar antiparallel  $\beta$ -sheet,<sup>30</sup> which has a different spectrum when compared with the twisted  $\beta$ -sheets normally observed in proteins. While a negative couplet at L1 is expected due to the presence of a random coil state,<sup>31,32</sup> the under-stabilization of PPII conformations<sup>33</sup> in MD simulations of unfolded peptides<sup>34,35</sup> may cause L1 to display a positive couplet, as noted in a recent study.<sup>33</sup> Our simulations indicate that only 2% of conformations exist in the PPII state at L1. Newer force fields,<sup>34,35</sup> which have been optimized to accurately calculate properties for unfolded peptides, may be used to acquire more accurate VCD spectra.

In the 2DIR  $xyxy$  spectra (Figure 4b–f), there is a dominant diagonal peak at L1, L25, and L50, which splits into two peaks at L75 and L100. The cross peak labeled peak ‘A’ at  $(\omega_1, \omega_3) = (-1670, 1640) \text{ cm}^{-1}$  slightly enhances from L1 to L25, indicating that the helical structure tends to strengthen the chiral signals. Interestingly, this cross peak gradually fades when

the antiparallel  $\beta$ -sheet structure forms and basically disappears at L100.

A new cross peak at  $(-1630, 1650) \text{ cm}^{-1}$  clearly appears in the  $xyxy$  spectrum of the folded state (peak ‘B’, Figure 4f). This feature begins to occur at L75 as the  $\beta$ -sheet forms and is well-resolved at L100 when the antiparallel  $\beta$ -sheet structure forms. This cross peak is caused by the coupling between the low- and high-frequency  $\beta$ -sheet eigenstates and is well-resolved because it appears as a positive feature near the negative diagonal feature. This cross peak, which has also been observed in simulated chiral 2DIR spectra of the A $\beta$ 42 monomer,<sup>36</sup> can be a good indicator of  $\beta$ -sheets.

Our results have demonstrated how conformational evolution on the folding free-energy landscape can be monitored by the 2DIR spectroscopy. The simulated linear absorption spectra, nonchiral spectra, and chirality-induced 2DIR spectra illustrate the conformational changes during folding. In our simulations, the chiral 2DIR spectra displayed a very strong feature, indicating the formation of the folded antiparallel  $\beta$ -sheet. Whereas in the nonchiral signals the formation of the  $\beta$ -sheet is seen as a similar pattern in the spectra, the chiral signals display very interesting spectra features. The appearance of the  $\beta$ -sheet cross peak at  $(-1630, 1650) \text{ cm}^{-1}$  in the chiral spectra is better resolved than the cross peak in the nonchiral spectra due to the opposite signs of the overlapping cross peak and diagonal feature. Comparing the chiral and nonchiral 2DIR spectra, we have found that the chiral signals are more sensitive when the structural changes. However, these signals are roughly 1000 times weaker than their nonchiral counterparts and have not yet been observed in experiment. In the chiral 2DIR experiments, a typical box-car or pump–probe geometry may be used. A highly sensitive detector could be achieved by upconverting the signal to the visible and detecting using a charge-coupled device.<sup>37</sup> Nevertheless, chiral 2DIR spectroscopy is a promising technique for studying fast protein folding with improved structural and temporal resolution.

## ■ ASSOCIATED CONTENT

### ● Supporting Information

List of native contact of peptide Beta3s and a 1-D free-energy profile with respect to RMSD from the native state structure. This material is available free of charge via the Internet at <http://pubs.acs.org>.

## ■ AUTHOR INFORMATION

### Corresponding Author

\*E-mail: [jin.wang.1@stonybrook.edu](mailto:jin.wang.1@stonybrook.edu).

### Notes

The authors declare no competing financial interest.

## ■ ACKNOWLEDGMENTS

The research leading to these results has received funding from the National Institutes of Health (grants GM059230 and GM091364) and the National Science Foundation (grant CHE-1058791). N.K.P. is supported by a National Science Foundation Graduate Research Fellowship. J.J. acknowledges the support of National Natural Science Foundation of China (NSFC) (no. 91221104). Z.Z.L. and J.W. thank the National Science Foundation for support.



## REFERENCES

- (1) Levy, Y.; Wolynes, P. G.; Onuchic, J. N. Protein Topology Determines Binding Mechanism. *Proc. Natl. Acad. Sci. U.S.A.* **2004**, *101*, 511–516.
- (2) Shoemaker, B. A.; Portman, J. J.; Wolynes, P. G. Speeding Molecular Recognition by Using the Folding Funnel: The Fly-Casting Mechanism. *Proc. Natl. Acad. Sci. U.S.A.* **2000**, *97*, 8868–8873.
- (3) Lai, Z. Z.; Lu, Q.; Wang, J. Exploring the Thermodynamic Landscape, Kinetics, and Structural Evolution of a Protein Conformational Transition with a Microscopic Double-Well Model. *J. Phys. Chem. B* **2011**, *115*, 4147–4159.
- (4) Zhuang, W.; Abramavicius, D.; Mukamel, S. Two-Dimensional Vibrational Optical Probes for Peptide Fast Folding Investigation. *Proc. Natl. Acad. Sci. U.S.A.* **2006**, *103*, 18934–18938.
- (5) Mukamel, S.; Abramavicius, D. Many-Body Approaches for Simulating Coherent Nonlinear Spectroscopies of Electronic and Vibrational Excitons. *Chem. Rev.* **2004**, *104*, 2073–2098.
- (6) Marai, C.; Mukamel, S.; Wang, J. Probing the Folding of Mini-Protein Beta3s by Two-Dimensional Infrared Spectroscopy: Simulation Study. *PMC Biophys.* **2010**, *3*, 8, 5–6.
- (7) de Alba, E.; Santoro, J.; Rico, M.; Jiménez, M. A. De Novo Design of a Monomeric Three-Stranded Antiparallel Beta-Sheet. *Protein Sci.* **1999**, *8*, 854–865.
- (8) Brooks, B. R.; Brooks, C. L., III; Mackerell, A. D., Jr.; Nilsson, L.; Petrella, R. J.; Roux, B.; Won, Y.; Archontis, G.; Bartels, C.; Boresch, S.; Caflisch, A.; et al. CHARMM: The Biomolecular Simulation Program. *J. Comput. Chem.* **2009**, *30*, 1545–1614.
- (9) Brooks, B. R.; Bruccleri, R. E.; Olafson, B. D.; States, D. J.; Swaminathan, S.; Karplus, M. CHARMM: A Program for Macromolecular Energy, Minimization, and Dynamics Calculations. *J. Comput. Chem.* **1983**, *4*, 187–217.
- (10) Dominy, B. N.; Brooks, C. L., III. Development of a Generalized Born Model Parameterization for Proteins and Nucleic Acids. *J. Phys. Chem.* **1999**, *103*, 3765–3773.
- (11) Yang, A. S.; Honig, B. Free Energy Determinants of Secondary Structure Formation: II. Antiparallel  $\beta$ -Sheets. *J. Mol. Biol.* **1995**, *252*, 366–376.
- (12) Bursulaya, B. D.; Brooks, L.; Folding, C. L. Free Energy Surface of a Three-Stranded  $\beta$ -Sheet protein. *J. Am. Chem. Soc.* **1999**, *121*, 9947–9951.
- (13) Ferrara, P.; Caflisch, A. Folding Simulation of a Three-Stranded Antiparallel  $\beta$ -Sheet Peptide. *Proc. Natl. Acad. Sci. U.S.A.* **2000**, *97*, 10780–10785.
- (14) Ryckaert, J. P.; Ciccotti, G.; Berendsen, H. Numerical Integration of the Cartesian Equations of Motion of a System with Constraints: Molecular Dynamics of N-Alkanes. *J. Comput. Phys.* **2009**, *23*, 327–341.
- (15) Zhuang, W.; Hayashi, T.; Mukamel, S. Coherent Multidimensional Vibrational Spectroscopy of Biomolecules; Concepts, Simulations and Challenges. *Angew. Chem., Int. Ed.* **2009**, *48*, 3750–3781.
- (16) Hayashi, T.; Zhuang, W.; Mukamel, S. Electrostatic DFT Map for the Complete Vibrational Amide Band of NMA. *J. Phys. Chem. A* **2005**, *109*, 9747–9759.
- (17) Torii, H.; Tatsumi, T.; Tasumi, M. Effects of Hydration on the Structure, Vibrational Wavenumbers, Vibrational Force Field and Resonance Raman Intensities of N-methylacetamide. *J. Raman Spectrosc.* **1998**, *29*, 537–546.
- (18) MacKerell, A. D., Jr.; Bashford, D.; Bellott, M.; Dunbrack, R. L., Jr.; Evanseck, J. D.; Field, M. J.; Fischer, S.; Gao, J.; Guo, H.; Ha, S.; et al. All-Atom Empirical Potential for Molecular Modeling and Dynamics Studies of Proteins. *J. Phys. Chem. B* **1998**, *102*, 3586–3616.
- (19) Krivov, S. V.; Muff, S.; Caflisch, A.; Karplus, M. One-Dimensional Barrier-Preserving Free-Energy Projections of a  $\beta$ -Sheet Miniprotein: New Insights into the Folding Process. *J. Phys. Chem. B* **2008**, *112*, 8701–8714.
- (20) Bagchi, S.; Falvo, C.; Mukamel, S.; Hochstrasser, R. M. 2D-IR Experiments and Simulations of the Coupling between Amide-I and Ionizable Side Chains in Proteins: Application to the Villin Headpiece. *J. Phys. Chem. B* **2009**, *113*, 11260–11273.
- (21) Hayashi, T.; Mukamel, S. Vibrational-Exciton Couplings for the Amide I, II, III, and A modes of Peptides. *J. Phys. Chem. B* **2007**, *111*, 11032–11046.
- (22) Lai, Z.; Preketes, N. K.; Mukamel, S.; Wang, J. Monitoring the Folding of Trp-Cage Peptide by Two-Dimensional Infrared (2DIR) Spectroscopy. *J. Phys. Chem. B* **2013**, *117*, 4661–4669.
- (23) Ganim, Z.; Chung, H.; Smith, A.; DeFlores, L.; Jones, K.; Tokmakoff, A.; Amide, I. Two-Dimensional Infrared Spectroscopy of Proteins. *Acc. Chem. Res.* **2007**, *41*, 432–441.
- (24) Baiz, C.; Peng, C.; Reppert, M.; Jones, K.; Tokmakoff, A. Coherent Two-Dimensional Infrared Spectroscopy: Quantitative Analysis of Protein Secondary Structure in Solution. *Analyst* **2012**, *137*, 1793–1799.
- (25) Smith, A. W.; Chung, H. S.; Ganim, Z.; Tokmakoff, A. Residual Native Structure in a Thermally Denatured Beta-Hairpin. *J. Phys. Chem. B* **2005**, *109*, 17025–17027.
- (26) Smith, A. W.; Tokmakoff, A. Probing Local Structural Events in Beta-Hairpin Unfolding with Transient Nonlinear Infrared Spectroscopy. *Angew. Chem., Int. Ed.* **2007**, *46*, 7984–7987.
- (27) Wang, J.; Chen, J.; Hochstrasser, R. M. Local Structure of  $\beta$ -Hairpin Isotopomers by FTIR, 2D IR, and Ab Initio Theory. *J. Phys. Chem. B* **2006**, *110*, 7545–7555.
- (28) Wang, J.; Zhuang, W.; Mukamel, S.; Hochstrasser, R. Two-Dimensional Infrared Spectroscopy as a Probe of the Solvent Electrostatic Field for a Twelve Residue Peptide. *J. Phys. Chem. B* **2008**, *112*, 5930–5937.
- (29) Jiang, J.; Mukamel, S. Two-Dimensional Near-Ultraviolet Spectroscopy of Aromatic Residues in Amyloid Fibrils: a First Principles Study. *Phys. Chem. Chem. Phys.* **2011**, *13*, 2394–2400.
- (30) Hilario, J.; Kubelka, J.; Syud, F. A.; Gellman, S. H.; Keiderling, T. A. Spectroscopic Characterization of Selected  $\beta$ -Sheet Hairpin Models. *Biopolymers* **2002**, *67*, 233–236.
- (31) Keiderling, T. A. Protein and Peptide Secondary Structure and Conformational Determination with Vibrational Circular Dichroism. *Curr. Opin. Chem. Biol.* **2002**, *6*, 682–688.
- (32) Kubelka, J.; Bour, P.; Silva, R. A.; Gangani, D.; Decatur, S. M.; Keiderling, T. A. *Chirality: Physical Chemistry*; American Chemical Society: Washington, DC, 2002; Chapter 5, pp 50–64.
- (33) Verbaro, D.; Ghosh, I.; Nau, W. M.; Schweitzer-Stenner, R. Discrepancies between Conformational Distributions of a Polyalanine Peptide in Solution Obtained from Molecular Dynamics Force Fields and Amide I' Band Profiles. *J. Phys. Chem. B* **2010**, *114*, 17201–17208.
- (34) Best, R. B.; Hummer, G. Optimized Molecular Dynamics Force Fields Applied to the Helix-Coil Transition of Polypeptides. *J. Phys. Chem. B* **2009**, *113*, 9004–9015.
- (35) Best, R. B.; Zhu, X.; Shim, J.; Lopes, P. E. M.; Mittal, J.; Feig, M.; MacKerell, A. D. Optimization of the Additive CHARMM All-Atom Protein Force Field Targeting Improved Sampling of the Backbone  $\varphi$ ,  $\psi$  and Side-Chain  $\chi_1$  and  $\chi_2$  Dihedral Angles. *J. Chem. Theory Comput.* **2012**, *8*, 3257–3273.
- (36) Zhuang, W.; Sgourakis, N. G.; Li, Z.; Garcia, A. E.; Mukamel, S. Discriminating early stage A $\beta$ 42 monomer structures using chirality-induced 2DIR spectroscopy in a simulation study. *Proc. Natl. Acad. Sci. USA* **2010**, *107* (36), 15687–15692.
- (37) Nee, M. J.; McCanne, R.; Kubarych, K. J.; Joffe, M. Two-Dimensional Infrared Spectroscopy Detected by Chirped Pulse Upconversion. *Opt. Lett.* **2007**, *32*, 713–715.